

1 Dear Editor,

2 Thanks for giving us an opportunity to revise our manuscript (acp-2019-1045). We appreciate your positive and con-
3 structive comments. We have studied these comments carefully and make revisions on the manuscript. These com-
4 ments and the corresponding replies are listed below.

5 The **comments** are highlighted by gray. The symbol "»" quotes the original texts in the manuscript. Followed by the
6 comments are our responses and revisions in the manuscript. Some important revisions are colored by red. The tracked
7 change is attached at the end of this file.

8 With regards,

9 Shuqi Yan, Bin Zhu*, and all co-authors.

10

11

12 **1.** You need to emphasize what is the urbanization effect. You mention land use change in your model sensitivity ex-
13 periments. Does urbanization change the surface albedo, surface roughness, surface flux, ...etc? it need to be clearly
14 stated.

15 »Line 82: ... urbanization mainly refers to UHI and UDI associated with land use change and human activities...

16 Thank you for this valuable suggestion. The urbanization effect here refers to UHI and UDI induced by anthropogenic
17 heating and the land use change. The land use change includes the changes in corresponding surface properties, e.g.,
18 surface albedo, surface roughness, surface flux.

19 **Revision in line 82 (Introduction)**

20 urbanization mainly refers to UHI and UDI associated with land use change and human activities induced by an-
21 thropogenic heating and land use change with the corresponding surface property change (e.g., surface albedo,
22 surface roughness, surface flux).

23

24

25 **2.** Line 43, you say "The urban surface has a lower albedo". compared to what? to rural surface? why?.

26 Thank you for this valuable suggestion. We compare urban surface with rural surface. The albedo is 0.15 for urban
27 surface and 0.20 for rural surface in the WRF model setting.

28 **Revision in line 44 (Introduction)**

29 The urban surface has a lower albedo than do rural surface.

30

31 **3.** Line 60-61. "The aerosol indirect effect on clouds..." but here in the context you are talking about aerosol effect on
32 fog, not on clouds.

33 >>Line 60-61. The aerosol indirect effect **on cloud** is addressed as one of the most uncertain factors in the IPCC report.
34 Aerosol concentration has a two-fold effect on fog, which is called as the boomerang pattern (Koren et al., 2008).

35 Thank you for this valuable suggestion. We have corrected this sentence.

36 **Revision in line 60-63 (Introduction)**

37 The aerosol indirect effect on cloud is addressed as one of the most uncertain factors in the IPCC report. **This ef-**
38 **fect on fog is also complex and two-fold**, which is determined by aerosol concentration.

39

40 **4.** WRF-Chem. Please give the full name when it is first time mentioned in the paper.

41 Thank you for this valuable suggestion. We have given the full name “Weather Research and Forecasting with Chem-
42 istry” in Abstract and Introduction.

43 **Revision in line 20 (Abstract)**

44 ...a dense radiation fog event in East China in January 2017 was reproduced by the **Weather Research and Fore-**
45 **casting with Chemistry** (WRF-Chem) model.

46 **Revision in line 76 (Introduction)**

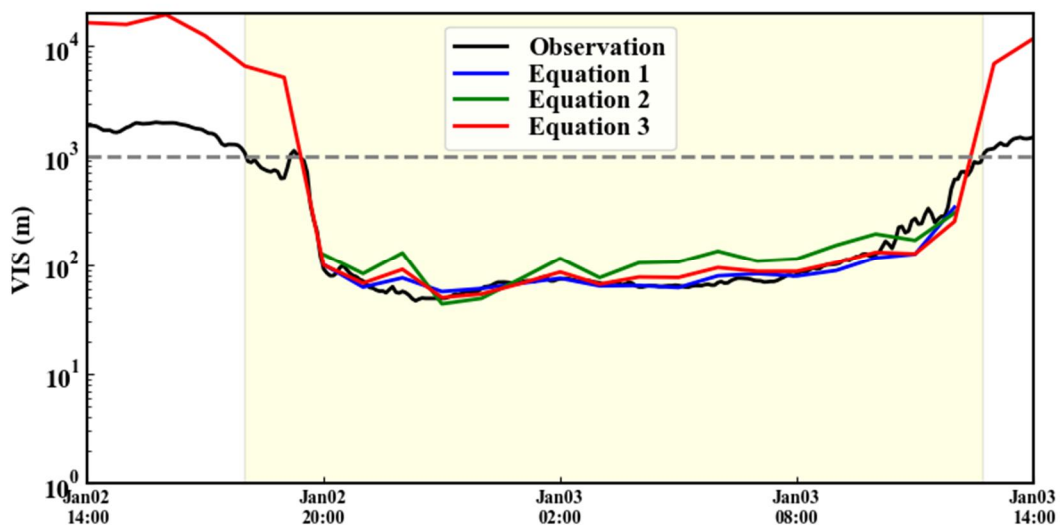
47 ...by an online-coupled synoptic and air quality model, Weather Research and Forecasting with Chemistry
48 (WRF-Chem).

49

50 **5.** Line 151 "figure not show". I'd like you to show the figure and put it in supplement.

51 >>Lines 151: During fog period (Fig. 4 shaded zone), the three methods nearly yield the same results (figure not
52 shown).

53 Thank you for this valuable suggestion. We did not show the visibility calculated by the three parameterization meth-
54 ods (corresponding to Equations 1 to 3). We have added Fig. S1 in the supplement.



56 Figure S1. Comparisons of VIS calculated by Equations 1, 2 and 3. The fog period (observed VIS < 1 km and RH >
57 90 %) is shaded with light yellow. Note that Equations 1 and 2 only consider the extinction by fog water, while Equa-
58 tion 3 considers the extinction by fog water and aerosols.

59

60

61 **6.** Line 168. "We assume that urbanization could have..." I'd change the sentence to something like "We hypothesize
62 that ..."

63 Thank you for this valuable suggestion. We have corrected this sentence.

64 **Revision in line 170 (Section 3.1.2)**

65 We **hypothesize** that urbanization could have....

67 **7.** Line 207. The first time "boomerang pattern" occurs please explain it. I know that you explain it later.

68 Thank you for this valuable suggestion. We think that the term "boomerang pattern" is not very common. In case the
69 readers might get confused, we avoid this term and change the corresponding expressions.

70 **Revision in line 61-63 (Introduction)**

71 The aerosol indirect effect on cloud is addressed as one of the most uncertain factors in the IPCC report. This ef-
72 fect on fog is also complex and **two-fold**, which is determined by aerosol concentration.....

73 **Revision in line 209 (Section 3.4)**

74 It is probable that the current pollution level of China always promotes fog occurrence. To testify whether the
75 $u0e3$ is below the transition point of **the boomerang pattern** that **suppresses fog**...

76 **Revision in line 214 (Section 3.4)**

77 All the **The variation shape of the** four parameters **show the boomerang pattern**, which demonstrates that the model is
78 able to simulate the dual effects of aerosols.

79 **Revision in line 293 (Conclusions)**

80 Further sensitivity experiments show that the current pollution level in China could be still below the **transition point of**
81 **boomerang pattern** **critical aerosol concentration** that suppresses fog.

82

83

84 **8.** Line 244. "boundary layer and advection tendencies is equal to the LWC distribution". The sentence is not correct.
85 how can tendencies equal to state (LWC). tendencies are changes of state (e.g., LWC).

86 »Line 244: The sum of microphysical (condensation/evaporation and sedimentation), boundary layer and advection
87 tendencies is equal to the LWC distribution.

88 Thank you for this valuable suggestion. The tendencies are changing rates ($\frac{\Delta \text{LWC}}{\Delta t}$) in unit of g/kg h⁻¹. We aim to express
89 that summing the integral of these tendencies with respect to time ($\sum \frac{\Delta \text{LWC}}{\Delta t} \Delta t$) equals to LWC, where Δt is the model
90 output time interval (1 hour).

91 **Revision in line 245-247 (Section 3.5)**

92 Summing the integral of microphysical (condensation/evaporation and sedimentation), boundary layer and advec-
93 tion tendencies with respect to time equals to the LWC distribution.

94

95 **9.** Figures 10 and 11. here the unit of tendencies should be g/kg/time.

96 Thank you for this valuable suggestion. We have changed the unit to be g kg⁻¹ h⁻¹ in Fig. 10, Fig. 11, Fig. S3 and Fig.
97 S4.

To what extents do urbanization and air pollution affect fog?

Shuqi Yan^{1,2,3,4}, Bin Zhu^{1,2,3,4,*}, Yong Huang^{5,6}, Jun Zhu⁷, Hanqing Kang^{1,2,3,4}, Chunsong Lu^{1,2,3,4}, Tong Zhu⁸

¹Collaborative Innovation Center on Forecast and Evaluation of Meteorological Disasters, Nanjing University of Information Science & Technology, Nanjing, China

²Key Laboratory for Aerosol-Cloud-Precipitation of China Meteorological Administration, Nanjing University of Information Science & Technology, Nanjing, China

³Key Laboratory of Meteorological Disaster, Ministry of Education (KLME), Nanjing University of Information Science & Technology, Nanjing, China

⁴Special test field of National Integrated meteorological observation, Nanjing University of Information Science & Technology, Nanjing, China

⁵Anhui Meteorology Institute, Key Lab of Atmospheric Science and Remote Sensing Anhui Province, Hefei 230031, China

⁶Shouxian National Climatology Observatory, Shouxian 232200, China

⁷Xiangshan Meteorological Bureau, Xiangshan 315700, China

⁸IMSG at NOAA/NESDIS/STAR, 5830 University Research Ct., College Park, MD 20740, USA

Correspondence to: Bin Zhu (binzhu@nuist.edu.cn)

Abstract. The remarkable development of China has resulted in rapid urbanization (urban heat island and dry island) and severe air pollution (aerosol pollution). Previous studies demonstrate that these two factors have either suppressing or promoting effects on fog, but what are the extents of their individual and combined effects? In this study, a dense radiation fog event in East China in January 2017 was reproduced by the [Weather Research and Forecasting with Chemistry](#) (WRF-Chem) model, and the individual and combined effects of urbanization and aerosols on fog (indicated by liquid water content (LWC)) are quantitatively revealed. Results show that urbanization inhibits low-level fog, delays its formation and advances its dissipation due to higher temperatures and lower saturations. In contrast, upper-level fog could be enhanced because of the updraft-induced vapour convergence. Aerosols promote fog by increasing LWC, increasing droplet concentration and decreasing droplet effective radius. Further experiments show that the current pollution level in China could be still below the critical aerosol concentration that suppresses fog. Urbanization influences fog to a larger extent than do aerosols. When urbanization and aerosol pollution are combined, the much weaker aerosol promoting effect is counteracted by the stronger urbanization suppressing effect on fog. Budget analysis of LWC reveals that urban development (urbanization and aerosols) alters LWC profile and fog structure mainly by modulating condensation/evaporation process. Our results infer that urban fog will be further reduced if urbanization keeps developing and air quality keeps deteriorating in the future.

31 **1 Introduction**

32 During the past five decades, China has achieved remarkable developments, accompanied by strong anthropogenic activities
33 (rapid urbanization and severe air pollution). Urbanization and air pollution have significantly affected climate change,
34 monsoons, air quality, fog, clouds and precipitation (e.g., Li et al., 2016; Li et al., 2017). Previous studies have linked the
35 changes in clouds and precipitation to urbanization and aerosols. Urbanization destabilizes the boundary layer, which trig-
36 gers strong updrafts and invigorates convection (e.g., Rozoff et al., 2003; Shepherd, 2005). Aerosols modify the macroscopic,
37 microphysics, thermodynamics and radiative properties of clouds through complicated pathways, which are called as aero-
38 sol-radiation and aerosol-cloud interactions and have been systematically reviewed by Fan et al. (2016), Rosenfeld et al.
39 (2014), Tao et al. (2012), etc. Fog can be viewed as a cloud (Leng et al., 2014) that occurs near the surface. Land use features
40 and aerosol properties may instantly affect fog, so fog is more sensitive to anthropogenic activities than other types of clouds
41 are (Zhu and Guo, 2016). Previous studies have analysed the effects of urbanization and aerosols on fog, mostly in segregat-
42 ed manners.

43 Urbanization is featured with urban heat island (UHI) and dry island (UDI) effects. The urban surface has a lower albedo
44 than do rural surface, which reduces the reflected solar radiation and enhances heat storage. Urban expansion decreases the
45 coverage of cropland, water bodies and forestland, which reduces the sources of water vapour. As a result, urban areas com-
46 monly experience higher temperatures and lower vapour contents. These conditions induce a lower relative humidity that is
47 unfavourable for fog formation (Gu et al., 2019). In the long-term scale, urban fog days are reported to decrease significantly
48 (e.g., Guo et al., 2016; LaDochy, 2005; Sachweh and Koepke, 1995; Shi et al., 2008; Yan et al., 2019). Although UHI and
49 UDI inhibit near-surface fog, the upward motions can promote upper-level fog (Li et al., 2011; Niu et al., 2010b). Surface
50 roughness and thermal circulation cause strong updrafts (Rozoff et al., 2003), which transfer water vapour aloft and cause
51 wet island phenomenon in the upper-level (Kang et al., 2014). The fog at that altitude may be subsequently enhanced.

52 Aerosols exert sophisticated impacts on fog through direct (radiation) effects and indirect (microphysical) effects (Khain and
53 Pinsky, 2018). Aerosols attenuate shortwave radiation, influencing PBL structure and the vertical profile of moisture and
54 aerosols (Tie et al., 2017, 2019), which can alter the formation and dissipation condition of fog. Scattering aerosols block
55 downwelling solar radiation in the daytime, thus delaying the dissipation and elongating the duration of fog (Shi et al., 2008;
56 Maalick et al., 2016). Although they increase downwelling longwave radiation at night, scattering aerosols have negligible
57 effects on the fog formation time (Stolaki et al., 2015; Maalick et al., 2016). The role of absorbing aerosols like black carbon
58 (BC) on fog depends on its residence height. If BC resides above the fog layer, BC causes a dome effect (Ding et al., 2016)
59 which blocks solar radiation and prevents the dissipation of fog (Bott, 1991). If BC resides within the fog layer, BC heats fog
60 droplets and accelerates the dissipation of fog (Maalick et al., 2016). The aerosol indirect effect on cloud is addressed as one

of the most uncertain factors in the IPCC report (IPCC, 2013). This effect on fog is also complex and two-fold, which is determined by aerosol concentration has a two-fold effect on fog, which is called as the boomerang pattern (Koren et al., 2008). Under saturation conditions, increasing aerosols commonly result in more CCNs. It promotes activation and condensation, yielding more but smaller droplets and increasing cloud water content (Fan et al., 2018; Rosenfeld et al., 2008). These changes have two kinds of positive feedback on fog (Maalick et al., 2016): more droplets cause stronger radiative cooling at fog top and enhance condensation (Jia et al., 2018); smaller droplet size inhibits sedimentation and the depletion of cloud water (Zhang et al., 2014). However, if aerosol concentration exceeds a certain threshold, this promoting effect disappears (Quan et al., 2011) or even turns into a suppressing effect due to the strong vapour competition (Guo et al., 2017; Koren et al., 2008; Liu et al., 2019; Rangognio, 2009; Wang et al., 2015). Additionally, large-scale aerosol pollution can change weather patterns and affect large-scale fog formation conditions (Niu et al., 2010a). Ding et al. (2019) found that the dome effects of BC induce a land-sea thermal contrast and generate a cyclonic anomaly over coastal areas. This anomaly results in more vapor transported inland and strengthened advection-radiation fog.

Our recent observational work (Yan et al., 2019) indicated a decreasing trend in fog days, and the inhibiting effects of urbanization outweigh the promoting effects of aerosols on fog during the mature urbanization stage. This study aims to quantitatively confirm the roles of urbanization and aerosols in a dense fog event by an online-coupled synoptic and air quality model, Weather Research and Forecasting with Chemistry (WRF-Chem). This event is a radiation fog event with weak synoptic forcing (detailed in Sect. 3.1), so the effects of urbanization and aerosols should be obvious. Determining the quantitative extents of urbanization effect, aerosol effect and their combined effect is an interesting topic, which has barely been studied previously to the best of our knowledge. This work is expected to facilitate the understanding of how anthropogenic activities affect the natural environment, fog (cloud) physics and aerosol-cloud interactions near the surface.

In this study, urbanization mainly refers to UHI and UDI-associated with land use change and human activities induced by anthropogenic heating and land use change with the corresponding surface property change (e.g., surface albedo, surface roughness, surface flux), excluding the increasing aerosol pollution caused by urban expansion. Air pollution refers to aerosols and is indicated by anthropogenic emissions because aerosol concentration is highly proportional to emission intensity. Liquid water content (LWC) and cloud/fog droplet number concentration (N_d) are two important parameters representing fog intensity and visibility. Following previous studies (e.g., Ding et al., 2019; Gu et al., 2019; Jia et al., 2018; Maalick et al., 2016; Yang et al., 2018), we use LWC as the indicator of fog to reveal different characteristics of fog in different experiments. This study is organized as follows. The data, model and methods are described in Sect. 2. Section 3.1 overviews the fog event and provides preliminary evidence of how urban development affects fog. Section 3.2 evaluates the model performance. Sections 3.3 to 3.5 analyse the urbanization, aerosol and combined effects on fog. Section 3.6 discusses the rationality and reliability of the results. Section 4 concludes the findings of this study.

92 **2 Data, model and methods**

93 **2.1 Data**

94 The first data are the hourly automatic weather station data from the Shouxian National Climate Observatory (SX; 32.4° N,
95 116.8° E, 23 m) that are used to evaluate the model performance. SX is a rural site surrounded by vast croplands and is ap-
96 proximately 30 km away from the nearest large city, Huainan (Fig. 1b). The data include horizontal visibility, temperature,
97 relative humidity, wind direction and speed. The second data are the Himawari 8 satellite data that are used to represent fog
98 area (<https://www.eorc.jaxa.jp/ptree/index.html>). Fog area is mainly indicated by the albedo at three visible bands: red (band
99 3, 0.64 μm), green (band 2, 0.51 μm) and blue (band 1, 0.47 μm). The third data are the 3-hourly data from the Meteorologi-
100 cal Information Comprehensive Analysis and Process System (MICAPS) (Li et al., 2010) that are also used to represent the
101 fog area. The fourth data are the land use data from the Moderate Resolution Imaging Spectroradiometer Land Cover Type
102 Version 6 data (MCD12Q1; <https://lpdaac.usgs.gov/products/mcd12q1v006>) in the year of 2017, the same as the simulation
103 period. The data are resampled from 500 m to 30 arc-seconds (approximately 1 km) and used to replace the geological data
104 of the WRF model.

105 **2.2 Model configuration**

106 The model used in this study is the WRF-Chem (V3.9.1.1) model. It is an online-coupled mesoscale synoptic and air quality
107 model that considers the sophisticated interactions among various dynamic, physical and chemical processes (Chapman et al.,
108 2009; Fast et al., 2006). WRF or WRF-Chem has been successfully used in simulating fog events (Jia and Guo, 2012; Jia and
109 Guo, 2015; Jia et al., 2018) and exploring aerosol-cloud interactions (Fan et al., 2018). Two nest domains are set up (Fig. 1).
110 The d01 domain has a size of 217×223 grids and a resolution of 6 km, covering the entire fog area of this event (Fig. 2a).
111 The d02 domain has a size of 115×121 grids and a resolution of 2 km, covering SX and the adjacent areas. The land use data
112 are replaced by MCD12Q1 data, which represent the latest condition.

113 Fog simulation is highly sensitive to vertical grids (Gultepe et al., 2007). A fine vertical resolution with a proper lowest
114 model level can better resolve turbulences, thus yielding a reasonable fog structure (Yang et al., 2019). Here, 42 vertical lev-
115 els are established with the first five η values of 1.000, 0.999, 0.998, 0.997, 0.996. There are 25 levels below the boundary
116 layer (approximately 1500 m), and the lowest model level is approximately 8 m.

117 Fog simulation is also sensitive to physical schemes (Gu et al., 2019). Through numerous experiments, radiation, micro-
118 physics and boundary schemes are found to significantly influence the model performance, and the boundary layer scheme
119 plays a decisive role (Naira Chaouch et al., 2017). The radiation schemes are the RRTM longwave scheme and the Goddard

shortwave scheme. The microphysical scheme is the Morrison double-moment scheme (Morrison et al., 2005). The boundary layer scheme is the YSU 1.5-order closure non-local scheme, which yields better results than do any other schemes. The major schemes are listed in Tab. 1.

The model is driven by the highest resolution product (0.125° , approximately 13 km) of ECMWF data (<https://apps.ecmwf.int/datasets/data/interim-full-daily/levtype=sfc/>). The anthropogenic emissions are derived from the Multi-resolution Emission Inventory for China (MEIC) database (<http://www.meicmodel.org>). The simulation starts at 2017-01-01 08:00 and ends at 2017-01-03 14:00, with the first 24 hours as the spin-up period (all the times here are in local time).

2.3 Sensitivity experiments

The study site is SX because only its visibility is observed hourly and is a multiple of 1 m, which is suitable for evaluating the model performance. To investigate the effects of urbanization and aerosols on fog, we change the land use and emission intensity around SX. Four experiments, i.e., u0e0, u3e0, u0e3 and u3e3 are designed. The u0e0 is the base experiment, with no urbanization and weak emission at SX. The u3e0 is set as the urbanization condition. The u0e3 is set as the polluted condition. The u3e3 is set as the urban development condition (urbanization and pollution coexist). The experiment settings are listed in Tab. 2.

On the setting of urbanized condition, we replace the land use of SX as that of Hefei, the most urbanized city and the capital of Anhui Province. The downtown of Hefei has a built area of approximately 570 km^2 . Therefore, the 11×13 box centered on SX (572 km^2) is replaced by urban surface in the u3e0 and u3e3 experiments to represent the urbanization condition.

The downtown of Hefei has much higher emissions than SX. For example, the PM2.5 emission rate of Hefei is 40 times higher than that of SX. To represent the polluted condition, the emission intensity of the aforementioned box is set to be equal to that of downtown Hefei in the u0e3 and u3e3 experiments.

2.4 Calculating visibility

The LWC is the proxy of fog as mentioned above. Since the LWC is not observed, and visibility (VIS) is related to LWC, the VIS is used to assess the model performance. VIS is not diagnosed by the model and can be parameterized by the function of LWC, N_d or droplet effective radius (R_e). Equation 1 (Kunkel, 1983) and 2 (Gultepe et al, 2006) are two parameterization methods.

$$\text{VIS[m]} = 27 \text{LWC[g cm}^{-3}\text{]}^{-0.88} \quad (1)$$

$$VIS[m] = 1002(LWC[g\ cm^{-3}] \cdot N_d[cm^{-3}])^{-0.6473} \quad (2)$$

146 Another parameterization method is based on the Mie theory (Gultepe et al., 2017). VIS is inverse proportional to atmos-
 147 pheric extinction at visible wavelength. The extinction coefficient of cloud water (β_c) is

$$\beta_c [km^{-1}] = \frac{3Q_{ext}\rho_a LWC}{4\rho_w R_e} \times 10^6 \quad (3)$$

148 where ρ_a (ρ_w) is the air (water) density in $kg\ m^{-3}$, LWC is in $g\ kg^{-1}$, R_e is in μm , and Q_{ext} is the extinction efficiency, which is
 149 assumed to be 2 for cloud droplets.

150 The atmospheric extinction (β) is also largely contributed by aerosols (β_a) and other types of hydrometeors. The model diag-
 151 noses β_a at 550 nm. No other types of hydrometeors occur in this fog case, so we assume $\beta = \beta_a + \beta_c$. Then VIS is determined
 152 by the Koschmieder rule (Koschmieder, 1924): $VIS[m] = 3.912/\beta[km^{-1}] \times 1000$.

153 During fog period (Fig. 4 shaded zone), the three methods nearly yield the same results ([Fig. S1 figure not shown](#)), so the last
 154 method is used to calculate the simulated VIS.

155 3 Results and discussions

156 3.1 Overview of the fog event

157 3.1.1 Formation condition and lifetime

158 From 01 to 06 January 2017, East China is dominated by zonal circulation, with weak trough, ridge, pressure gradient and
 159 atmospheric diffusion (Zhang and Ma, 2017). Under this stable weather pattern, the accumulation of pollutants and water
 160 vapour promotes the occurrence of fog-haze events. From the evening of 02 January to the noon of 03 January, a dense fog
 161 event occurs in wide regions of East China. The fog reaches its peak at 08:00 03 January, covering south Hebei, east Henan,
 162 west Shandong, Anhui, Jiangsu and Shanghai (Fig. 2a). Figure 4a shows the temporal variation of visibility at SX. The fog
 163 forms at 18:00 02 January and dissipates at 12:40 03 January. This is a radiation fog which is promoted by strong radiative
 164 cooling at night and weak easterly water vapour transport from northwest Pacific (Zhu et al., 2019).

165 3.1.2 Preliminary evidence of urban development affecting fog

166 Lee (1987) and Sachweh and Koepke (1995) observed "fog holes" over urban areas on satellite images. Here, fog hole means

167 the low liquid water path (LWP) region within the fog region, which is visualized as pixels with weak fog (high visibility) or
168 clear sky surrounded by dense fog. These holes demonstrate that urban development (urbanization and aerosols) has a clearing
169 effect on fog. In this fog event, fog holes are also present over urban areas on the Himawari 8 image at 11:00 03 January
170 (Fig. 3). We assumehypothesize that urbanization could have profound effects on fog by reducing the LWP or advancing the
171 dissipation of fog, and the role of aerosols on fog is weaker than that of urbanization.

172 **3.2 Model evaluation and simulations**

173 The model performance is evaluated by comparing the fog spatial coverage. Satellite cloud image and modelled LWP ($>2 \text{ g m}^{-2}$) can represent the observed and simulated fog zone, respectively (Jia et al., 2018). Figure 2 shows the Himawari 8 visible
174 cloud image and the simulated LWP distribution at 08:00. The light white pixels and light red dots indicate the observed fog
175 area. The model well captures the fog in south Hebei, east Henan, west Shandong, Anhui, Jiangsu and Shanghai.
176

177 The model performance is also evaluated by comparing the visibility and other basic parameters at the SX site (Fig. 4). Seen
178 from the visibility, the simulated fog forms at 19:30, 1.5 h later than the observation, and dissipates at 12:20, 30 min earlier
179 than the observation. During the fog period, the simulated visibility agrees well with the observation. The other parameters
180 such as temperature, wind speed and relative humidity are also effectively reproduced by the model, with relative small
181 RMSEs of 0.8 K, 0.7 m/s and 5.9 %, respectively. Overall, the model well captures the spatial feature and temporal evolution
182 of the fog.

183 **3.3 Urbanization effects**

184 From different sensitivity experiments (u3e0, u0e3 and u3e3), we can deduce the extents of the separate or combined effects
185 of urbanization and aerosols on fog. Figure 5 compares the LWC between u0e0 and u3e0. The general results are: (1) Before
186 02:00, urbanization leads to a decreasing LWC in all layers. Fog forms on the surface at 22:30 in u3e0, 3 h later than in u0e0.
187 (2) After 02:00, the LWC decreases in the low-level while it increases in the upper-level. Fog dissipates at 10:50 in u3e0, 1.5
188 h earlier than in u0e0. To better explain the LWC difference, its profiles are shown in Fig. 6. At 23:00, although fog has
189 formed in u3e0, the fog is rather weak compared with u0e0, which is caused by the higher temperature (Fig. 6f) and lower
190 saturation associated with UHI and UDI. At 02:00, fog develops in u3e0, but its intensity (the value of LWC) cannot reach
191 the same level as that in u0e0.

192 An interesting phenomenon is the opposite change of LWC in the low-level and upper-level after 02:00. This phenomenon
193 can be explained by the role of updrafts. The increasing roughness length and extra warming in urban conditions could trig-
194 ger horizontal wind convergence (Fig. S4S2) and the enhanced updrafts (Fig. 5c). The stronger updrafts in u3e0 affect con-

195 densation via two possible pathways: (1) the vertical transport of vapour ($-w \frac{\partial q}{\partial z}$) and vertical convergence/divergence ($-q \frac{\partial w}{\partial z}$)
 196 redistribute water vapour and affect condensation; (2) the adiabatic cooling promotes condensation. The role of the first
 197 pathway is measured by vertical vapour flux divergence ($\frac{1}{g} \frac{\partial(qw)}{\partial z}$). At 05:00, u3e0 shows a stronger vapour convergence above
 198 110 m (Fig. 6h), and the LWC increases above 130 m (Fig. 6c). At 08:00, u3e0 shows a stronger vapour convergence above
 199 130 m (Fig. 6i), and the LWC increases above 170 m (Fig. 6d). Therefore, it is possible that the adiabatic cooling and up-
 200 draft-induced vapour flux convergence increase the vapour content and promote condensation in the upper-level, while the
 201 fog in the low-level is suppressed by the divergence of vapour flux. At 11:00, fog disappears at the ground in u3e0 likely due
 202 to the higher temperature (Fig. 6j). In summary, the UHI, UDI and updrafts alter the profile of LWC and reduce the LWP
 203 most of the time (Fig. 5c), and the decreasing LWP in the daytime can explain why fog holes occur above urban areas (Fig.
 204 3).

205 3.4 Aerosol effects

206 Figure 7 compares the LWC between u0e0 and u0e3. The formation time, dissipation time of fog and fog top show almost no
 207 changes. The LWC increases at almost all layers in the polluted condition. Accordingly, the LWP also increases (Fig. 7c). It
 208 is probable that the current pollution level of China always promotes fog occurrence. To testify whether the u0e3 is below
 209 the transition point ~~of the boomerang pattern that suppresses fog~~, eight additional experiments (D10, D7.5, D5, D2.5, M2.5,
 210 M5, M7.5 and M10) are performed. These experiments are the same as u0e3, except that the emissions around SX (the black
 211 box in Fig. 1b) are multiplied (the "M" prefix) or divided (the "D" prefix). For example, the name M2.5 means multiplying
 212 by 2.5; the name D10 means dividing by 10.

213 Figure 8 compares the LWC, N_d , R_e and LWP among the nine emission-variant experiments. ~~All the~~The variation shape of
 214 the four parameters show the boomerang pattern, which demonstrates that the model is able to simulate the dual effects of
 215 aerosols. Below u0e3, the four parameters monotonically vary with emission level or CCN concentration, indicating that
 216 aerosol pollution could always promote fog. This phenomenon is because stronger emissions produce more aerosols and
 217 CCN. Under saturation conditions, the larger amount of CCN boost activation and yield a higher N_d . The higher N_d reduces
 218 R_e and inhibits autoconversion and sedimentation (Twomey, 1977); thus, this situation decreases the depletion of fog water
 219 and increases the LWC. This promoting effect has been confirmed by previous model studies (e.g., Maalick et al., 2016; Sto-
 220 laki et al., 2015) and observations (e.g., Chen et al., 2012; Goren and Rosenfeld, 2012). The CCN_{0.1} concentration of u0e3
 221 (570 cm^{-3}) is lower than that of the turning point (experiment M2.5) (1349 cm^{-3}), possibly indicating that the current pollu-
 222 tion level in China (u0e3) is still located in the promoting regime rather than the suppressing regime of fog occurrence.

223 Rosenfeld et al. (2008) revealed that the turning point ~~of boomerang pattern~~ in convective clouds is CCN_{0.4} = 1200 cm^{-3} . The

CCN_{0.4} of u0e3 is 6023 cm⁻³, which seems to suppress fog. Aerosols affect convective clouds through two competing mechanisms: 1) invigorating convection by promoting vapour condensation. 2) suppressing convection by blocking solar radiation and reducing surface heat flux. Under polluted conditions (AOD>0.3 or CCN_{0.4}>1200 cm⁻³), the suppressing effect outweighs the invigoration effect, so the turning point occurs (Koren et al., 2008; Rosenfeld et al., 2008). This suppressing effect does not exist in fog because fog commonly formed at night. Therefore, the turning point in fog might occur later than that in convective clouds. In North China Plain where air pollution is thought to be more serious, a case study by WRF-Chem also indicates that fog properties (e.g., LWC, N_d and LWP) increase monotonically when emission intensity varies from 0.05-fold to 1-fold.

3.5 Combined effects of urbanization and aerosols

Figure 9 compares the LWC between u0e0 and u3e3. The u3e3-induced change is quite similar to but not the same as the u3e0-induced change. The time-height average of absolute change of LWC induced by u3e0, u0e3 and u3e3 are 0.120, 0.019, 0.124 g kg⁻¹, respectively. This result indicates that urbanization affects fog to a larger extent than do aerosols; when urbanization and aerosols are combined, the effect of aerosols is indiscernible. The LWP is also significantly suppressed in the daytime, and the promoting effect of aerosols in Fig. 7c is indiscernible in Fig. 9c. To further explain the changes in LWC, we perform budget analysis of the LWC to determine which physical processes are the dominant contributors.

In WRF, the budget of LWC is composed of the following items,

$$\frac{\partial q_c}{\partial t} = \underbrace{\left(u \frac{\partial}{\partial x} + v \frac{\partial}{\partial y} + w \frac{\partial}{\partial z} \right) q_c}_{\text{adv}} + \left(\frac{\partial q_c}{\partial t} \right)_{\text{PBL}} + \left(\frac{\partial q_c}{\partial t} \right)_{\text{micro}} + \left(\frac{\partial q_c}{\partial t} \right)_{\text{cumu}} \quad (4)$$

where q_c is LWC, and the subscripts denote advection, boundary layer, microphysical and cumulus processes, respectively.

The microphysical tendency is further decomposed into the following items,

$$\left(\frac{\partial q_c}{\partial t} \right)_{\text{micro}} = \left(\frac{\partial q_c}{\partial t} \right)_{\text{cold}} + \left(\frac{\partial q_c}{\partial t} \right)_{\text{auto}} + \left(\frac{\partial q_c}{\partial t} \right)_{\text{accr}} + \left(\frac{\partial q_c}{\partial t} \right)_{\text{sed}} + \left(\frac{\partial q_c}{\partial t} \right)_{\text{cond/evap}} \quad (5)$$

where the subscripts denote cold phase processes, autoconversion, accretion, sedimentation and condensation/evaporation, respectively.

All the processes regarding precipitation and cold phase (the cumu, cold, auto and accr subscripts) are not analysed because no precipitation occurs, and the temperature is above 0°C in the simulated fog (figure not shown). The sum Summing the

246 | integral of microphysical (condensation/evaporation and sedimentation), boundary layer and advection tendencies with respect to time is equal to ~~the LWC-distribution~~, so the contributions of other physical processes can be safely ignored.

248 | We can also infer that to what extents the various physical processes affect fog through the sensitivity experiments (u3e0,
249 | u0e3 and u3e3). Additional aerosols weakly influence these processes (Fig. S2-S3 right column) and subsequently result in
250 | weak LWC change (Fig. 7c). Compared with aerosols, urbanization effect is much more considerable (Fig. S3-S4 right col-
251 | umn); it dominantly accounts for the variation in physical tendencies from u0e0 to u3e3 (Fig. 10 right column). In u3e3 con-
252 | dition, urban development (urbanization and aerosols) induces different magnitude of changes in different physical tenden-
253 | cies. The relative magnitudes are 52.1, 38.3 and 9.6 % for the microphysical, boundary layer and advection processes, re-
254 | spectively, indicating that microphysics is most susceptible to urban development and contributes most to the LWC change.
255 | Among various microphysical processes, condensation/evaporation contributes most (72.7 %) to the change in microphysical
256 | tendency (Fig. 11 right column). The above results indicate that urban development affects the LWC mainly by modulating
257 | the condensation/evaporation process. Since u3e3 condition still witnesses higher temperatures and stronger updrafts (figure
258 | not shown), the notable variation in condensation/evaporation tendency induced by u3e3 can also be attributed to the pre-
259 | dominant role of UHI, UDI and updrafts. The mechanism has been analysed in Sect. 3.3.

260 | **3.6 Discussions**

261 | As mentioned above, urbanization influences fog to a larger extent than do aerosols; the LWC in fog does not vary substan-
262 | tially with pollution level. This section discusses the rationality and reliability of our results through mechanism analysis and
263 | observational evidence.

264 | The sensitivity of cloud properties to aerosols depends on aerosol concentration and saturation environment. In convective
265 | clouds with intense upward motions and high saturations, the response of cloud properties to additional aerosols is signifi-
266 | cant ("aerosol-limited regime") (Fan et al., 2018). However, in fog with much weaker updrafts and lower saturations, this
267 | response could be more sensitive to vapour content rather than aerosol concentration ("vapour-limited regime"). It possibly
268 | implies that the LWC in fog varies slightly with pollution level but considerably with saturation condition that related to ur-
269 | banization. Our results reveal that the time-height average LWC varies within the extent of 0.07 g kg^{-1} when emission inten-
270 | sity varies within two orders of magnitude (Fig. 8). This relative weak response of the LWC to pollution level is also report-
271 | ed by Jia et al. (2018).

272 | In terms of observational evidence, Yan et al. (2019) revealed that fog days in polluted regions of East China have decreased
273 | since the 1990s. Through quantitative analysis, the promoting effects of aerosols are weakening, while the suppressing ef-
274 | ffects of urbanization are enhancing and dominantly cause this decrease. Sachweh and Koepke (1995) also claimed that the

275 hindering effects of urbanization outweigh the promoting effects of aerosols on fog in southern Germany. Additionally, satel-
276 lite images present discernible fog holes above urban areas (Fig. 3) (Lee, 1987; Sachweh and Koepke, 1995). Therefore,
277 these observational evidence support the model results that the promoting effect of aerosols is counteracted by the hindering
278 effect of urbanization. We believe that the results can also be applied to other large cities in China because these cities com-
279 monly witness strong UHI, UDI and severe air pollution.

280 4 Conclusions

281 A dense radiation fog event occurred in East China from 02 to 03 January 2017. Satellite images show that fog holes occur
282 over urban areas, demonstrating the remarkable effects of urbanization and air pollution on fog. Hence, the mechanism is
283 investigated by the WRF-Chem model. The model well captures the spatial coverage and temporal evolution of the fog. Fur-
284 thermore, the separate and combined effects of urbanization (refers to UHI and UDI) and air pollution (refers to aerosols) on
285 fog (indicated by the LWC) are revealed, and the extents of these effects are quantitatively determined. Results show that:

286 Urbanization redistributes the LWC profile by the UHI, UDI effect and updrafts. The updrafts may be caused by surface
287 roughness and extra warming. The UHI and UDI suppress low-level fog, delay its formation by 3 h, and advance its dissipa-
288 tion by 1.5 h. However, the upper-level fog could be enhanced due to the updraft-induced adiabatic cooling and vapour flux
289 convergence. Urbanization reduces the LWP most of the time, and this reduction in the daytime can explain why fog holes
290 are present above urban areas on satellite images.

291 Aerosols promote fog mainly by changing microphysical properties. The increasing emissions (aerosol concentration) pro-
292 duce more CCN and fog droplets, which decreases R_e and inhibits sedimentation, thus leading to a higher LWC. Further sen-
293 sitivity experiments show that the current pollution level in China could be still below the ~~transition point of the boomerang~~
294 ~~pattern~~ critical aerosol concentration that suppresses fog. The macroscopic properties such as fog top and lifetime remain
295 nearly unchanged.

296 The role of urbanization far outweighs that of aerosols. Therefore, when they act together, the urbanization effect is domi-
297 nant, and the aerosol effect is indiscernible. Budget analysis of LWC shows that increasing aerosols influence various physi-
298 cal processes to a lesser extent, while urbanization influences these processes to a larger extent, eventually leading to a sub-
299 stantial LWC change in urban development condition (urbanization and aerosols). In this condition, the comparisons among
300 various physical processes reveal that microphysics dominates the change in LWC, and condensation/evaporation dominates
301 the change in microphysical tendency. This result highlights the importance of condensation/evaporation process in modu-
302 lating the LWC profile and fog structure.

303 Mechanism analysis and the observational evidence support our key finding that urbanization influences fog to a much larger
304 extent than do aerosol pollution. Therefore, we believe our results are reasonable and robust in radiation fog events without
305 strong synoptic forcings, and the results can also be applied to other large cities in China due to the similar urban develop-
306 ment patterns. This study is expected to facilitate a better understanding of how anthropogenic activities affect the natural
307 environment, fog (cloud) physics and aerosol-cloud interactions near the surface. We can also infer the future change of fog
308 occurrence. Under the traditional urban development pattern, i.e., urbanization keeps developing and air quality keeps dete-
309 riorating, urban fog occurrence will be further reduced.

310

311 *Code and data availability.* Some of the data repositories have been listed in Sect. 2. The other data, model outputs and
312 codes can be accessed by contacting Bin Zhu via binzhu@nuist.edu.cn.

313

314 *Author contributions.* SY performed the model simulation, data analysis and manuscript writing. BZ proposed the idea, su-
315 pervised this work and revised the manuscript. YH provided the observation data at the SX site. JZ processed the observation
316 data. HK offered helps to the model simulation. CL and TZ also contributed to the manuscript revision.

317

318 *Competing interests.* The authors declare that they have no conflict of interest.

319

320 *Acknowledgments.* We are grateful to the High Performance Computing Center of Nanjing University of Information Science
321 and Technology for doing the numerical calculations in this work on its blade cluster system. We thank American Journal
322 Experts (AJE) for the English language editing.

323

324 *Financial support.* This work is supported by the National Key Research and Development Program (2016YFA0602003)
325 and the National Natural Science Foundation of China (91544229, 41575148, 41605091).

326 **References**

327 Abdul-Razzak, H. and Ghan, S. J.: A parameterization of aerosol activation 3. Sectional representation, *J. Geophys. Res.*, 107,
328 AAC-1-AAC 1-6, <https://doi.org/10.1029/2001jd000483>, 2002.

- 329 Bott, A.: On the influence of the physico-chemical properties of aerosols on the life cycle of radiation fogs, *J. Aerosol. Sci.*, 21, 1–31,
330 <https://doi.org/10.1007/BF00119960>, 1991.
- 331 Chapman, E. G., Gustafson, W. I., Easter, R. C., Barnard, J. C., Ghan, S. J., and Pekour, M. S.: Coupling aerosol-cloud-radiative processes
332 in the WRF-Chem model: Investigating the radiative impact of elevated point sources, *Atmos. Chem. Phys.*, 9, 945–964,
333 <https://doi.org/10.5194/acp-9-945-2009>, 2009.
- 334 Chen, Y. C., Christensen, M. W., Xue, L., Sorooshian, A., Stephens, G. L., Rasmussen, R. M., and Seinfeld, J. H.: Occurrence of lower
335 cloud albedo in ship tracks, *Atmos. Chem. Phys.*, 12, 8223–8235, <https://doi.org/10.5194/acp-12-8223-2012>, 2012.
- 336 Di Vittorio, A. V. and Emery, W. J.: An automated, dynamic threshold cloud-masking algorithm for daytime AVHRR images over land,
337 *IEEE Trans. Geosci. Remote Sensing*, 40, 1682–1694, <https://doi.org/10.1109/TGRS.2002.802455>, 2002.
- 338 Ding, A. J., Huang, X., Nie, W., Sun, J. N., Kerminen, V. - M., Petäjä, T., Su, H., Cheng, Y. F., Yang, X. - Q., Wang, M. H., Chi, X. G.,
339 Wang, J. P., Virkkula, A., Guo, W. D., Yuan, J., Wang, S. Y., Zhang, R. J., Wu, Y. F., Song, Y., Zhu, T., Zilitinkevich, S., Kulmala, M.,
340 and Fu, C. B.: Enhanced haze pollution by black carbon in megacities in China, *Geophys. Res. Lett.*, 43, 2873–2879,
341 <https://doi.org/10.1002/2016gl067745>, 2016.
- 342 Ding, Q., Sun, J., Huang, X., Ding, A., Zou, J., Yang, X., and Fu, C.: Impacts of black carbon on the formation of advection–radiation fog
343 during a haze pollution episode in eastern China, *Atmos. Chem. Phys.*, 19, 7759–7774, <https://doi.org/10.5194/acp-19-7759-2019>,
344 2019.
- 345 Fan, J., Rosenfeld, D., Zhang, Y., Giangrande, S. E., Li, Z., and Machado, L. A. T.: Substantial convection and precipitation enhancements
346 by ultrafine aerosol particles, *Science*, 359, 411–418, <https://doi.org/10.1126/science.aan8461>, 2018.
- 347 Fan, J., Wang, Y., Rosenfeld, D., and Liu, X.: Review of Aerosol–Cloud Interactions: Mechanisms, Significance, and Challenges, *J. Atmos.
348 Sci.*, 73, 4221–4252, <https://doi.org/10.1175/JAS-D-16-0037.1>, 2016.
- 349 Fast, J. D., Gustafson, W. I., Easter, R. C., Zaveri, R. A., Barnard, J. C., Chapman, E. G., Grell, G. A., and Peckham, S. E.: Evolution of
350 ozone, particulates, and aerosol direct radiative forcing in the vicinity of Houston using a fully coupled meteorolo-
351 gy-chemistry-aerosol model, *J. Geophys. Res.*, 111, <https://doi.org/10.1029/2005jd006721>, 2006.
- 352 Goren, T. and Rosenfeld, D.: Satellite observations of ship emission induced transitions from broken to closed cell marine stratocumulus
353 over large areas, *J. Geophys. Res.-Atmos.*, 117, -, <https://doi.org/10.1029/2012JD017981>, 2012.
- 354 Gu, Y., Kusaka, H., van Doan, Q., and Tan, J.: Impacts of urban expansion on fog types in Shanghai, China: Numerical experiments by
355 WRF model, *Atmos. Res.*, 220, 57–74, <https://doi.org/10.1016/j.atmosres.2018.12.026>, 2019.
- 356 Gultepe, I., Tardif, R., Michaelides, S. C., Cermak, J., Bott, A., Bendix, J., Müller, M. D., Pagowski, M., Hansen, B., Ellrod, G., Jacobs, W.,
357 Toth, G., and Cober, S. G.: Fog Research: A Review of Past Achievements and Future Perspectives, *Pure Appl. Geophys.*, 164, 1121–
358 1159, <https://doi.org/10.1007/s00024-007-0211-x>, 2007.
- 359 Gultepe, I., Müller, M. D., and Boybeyi, Z.: A New Visibility Parameterization for Warm-Fog Applications in Numerical Weather Predic-
360 tion Models, *J. Appl. Meteorol. Climatol.*, 45, 1469–1480, <https://doi.org/10.1175/jam2423.1>, 2006.
- 361 Gultepe, I., Milbrandt, J. A., and Zhou, B.: Marine fog: A review on microphysics and visibility prediction, in: Koračin D., Dorman C. (eds)
362 Marine Fog: Challenges and Advancements in Observations, Modeling, and Forecasting, Springer, Cham, 50 pp., 2017.
- 363 Guo, J., Su, T., Li, Z., Miao, Y., Li, J., Liu, H., Xu, H., Cribb, M., and Zhai, P.: Declining frequency of summertime local-scale precipita-
364 tion over eastern China from 1970 to 2010 and its potential link to aerosols, *Geophys. Res. Lett.*, 44, 5700–5708,
365 <https://doi.org/10.1002/2017GL073533>, 2017.
- 366 Guo, T., Zhu, B., Kang, Z., Gui, H., and Kang, H.: Spatial and temporal distribution characteristic of fog days and haze days from
367 1960~2012 and impact factors over the Yangtze River Delta Region, *China Environmental Science*, 36, 961 – 969,
368 <https://doi.org/10.3969/j.issn.1000-6923.2016.04.001>, 2016. [in Chinese]
- 369 IPCC: Climate change 2013: The physical science basis, Contribution of Working Group I to the Fifth Assessment Report of the Intergov-
370 ernmental Panel on Climate Change, Cambridge University Press, Cambridge, United Kingdom and New York, NY, USA, 1585 pp.,
371 2013.

- 372 Jia, X. and Guo X.: Impacts of Anthropogenic Atmospheric Pollutant on Formation and Development of a Winter Heavy Fog Event, Chi-
373 nese Journal of Atmospheric Sciences, 36, 995– 1008, <https://doi.org/10.3878/j.issn.1006-9895.2012.11200>, 2012. [in Chinese]
- 374 Jia, X. and Guo, X.: Impacts of Secondary Aerosols on a Persistent Fog Event in Northern China, Atmospheric and Oceanic Science Let-
375 ters, 5, 401–407, <https://doi.org/10.1080/16742834.2012.11447022>, 2015.
- 376 Jia, X., Quan, J., Zheng, Z., Liu, X., Liu, Q., He, H., and Liu, Y.: Impacts of anthropogenic aerosols on fog in North China Plain, J. Ge-
377 ophys. Res.-Atmos., 124, 252–265, <https://doi.org/10.1029/2018jd029437>, 2018.
- 378 Kang, H., Zhu, B., Zhu, T., Sun, J., and Ou, J.: Impact of Megacity Shanghai on the Urban Heat-Island Effects over the Downstream City
379 Kunshan, Bound.-Layer Meteor., 152, 411–426, <https://doi.org/10.1007/s10546-014-9927-1>, 2014.
- 380 Khain, A. P. and Pinsky, M.: Modeling: A Powerful Tool for Cloud Investigation, in: Physical processes in clouds and cloud modeling,
381 Cambridge University Press, Cambridge, United Kingdom and New York, NY, USA, 98 pp., 2018.
- 382 Koren, I., Martins, J. V., Remer, L. A., and Afargan, H.: Smoke invigoration versus inhibition of clouds over the Amazon, Science, 321,
383 946–949, <https://doi.org/10.1126/science.1159185>, 2008.
- 384 Koschmieder, H.: Therie der horizontalen sichtweite, Beitr Phys.d.freien Atm, 12, 171–181, 1924.
- 385 Kunkel, B. A.: Parameterization of Droplet Terminal Velocity and Extinction Coefficient in Fog Models, J. Appl. Meteorol., 23, 34–41,
386 [https://doi.org/10.1175/1520-0450\(1984\)023<0034:PODTVA>2.0.CO;2](https://doi.org/10.1175/1520-0450(1984)023<0034:PODTVA>2.0.CO;2), 1983
- 387 LaDochy, S.: The Disappearance of Dense Fog in Los Angeles: Another Urban Impact?, Phys. Geogr., 26, 177–191,
388 <https://doi.org/10.2747/0272-3646.26.3.177>, 2005.
- 389 Lee, T. F.: Urban clear islands in California central valley fog, Mon. Weather Rev., 115, 1794–1796,
390 [https://doi.org/10.1175/1520-0493\(1987\)1152.0.CO;2](https://doi.org/10.1175/1520-0493(1987)1152.0.CO;2), 1987.
- 391 Leng, C., Zhang, Q., Zhang, D., Xu, C., Cheng, T., Zhang, R., Tao, J., Chen, J., Zha, S., and Zhang, Y.: Variations of cloud condensation
392 nuclei (CCN) and aerosol activity during fog-haze episode: a case study from Shanghai, Atmos. Chem. Phys., 14, 12499–12512,
393 <https://doi.org/10.5194/acp-14-12499-2014>, 2014.
- 394 Li, Y., Cao, L., Gao, S., and Luo, B.: The Current Stage and Development of MICAPS, Meteorological Monthly, 36, 50–55, 2010. [in Chi-
395 nese]
- 396 Li, Z., Guo, J., Ding, A., Liao, H., Liu, J., Sun, Y., Wang, T., Xue, H., Zhang, H., and Zhu, B.: Aerosol and boundary-layer interactions and
397 impact on air quality, Natl. Sci. Rev., 4, 810–833, <https://doi.org/10.1093/nsr/nwx117>, 2017.
- 398 Li, Z., Lau, W. K. M., Ramanathan, V., Wu, G., Ding, Y., Manoj, M. G., Liu, J., Qian, Y., Li, J., Zhou, T., Fan, J., Rosenfeld, D., Ming, Y.,
399 Wang, Y., Huang, J., Wang, B., Xu, X., Lee, S. S., Cribb, M., Zhang, F., Yang, X., Zhao, C., Takemura, T., Wang, K., Xia, X., Yin, Y.,
400 Zhang, H., Guo, J., Zhai, P. M., Sugimoto, N., Babu, S. S., and Brasseur, G. P.: Aerosol and monsoon climate interactions over Asia,
401 Rev. Geophys., 54, 866–929, <https://doi.org/10.1002/2015RG000500>, 2016.
- 402 Li, Z., Yang, J., Shi, C., and Pu, M.: Urbanization Effects on Fog in China: Field Research and Modeling, Pure Appl. Geophys., 169, 927–
403 939, <https://doi.org/10.1007/s00024-011-0356-5>, 2011.
- 404 Liu, H., Guo, J., Koren, I., Altaratz, O., Dagan, G., Wang, Y., Jiang, J. H., Zhai, P., and Yung, Y. L.: Non-Monotonic Aerosol Effect on
405 precipitation in Convective Clouds over tropical oceans. Sci. Rep., 9, 1–7, <https://doi.org/10.1038/s41598-019-44284-2>, 2019.
- 406 Maalick, Z., Kühn, T., Korhonen, H., Kokkola, H., Laaksonen, A., and Romakkaniemi, S.: Effect of aerosol concentration and absorbing
407 aerosol on the radiation fog life cycle, Atmos. Environ., 133, 26–33, <https://doi.org/10.1016/j.atmosenv.2016.03.018>, 2016.
- 408 Morrison, H., Curry, J. A., and Khorostyanov, V. I.: A new double-moment microphysics parameterization for application in cloud and
409 climate models. Part I: Description, J. Atmos. Sci., 62, 1665–1677, <https://doi.org/10.1175/JAS3446.1>, 2005.
- 410 Naira Chaouch, Marouane Temimi, Michael Weston, and Hosni Ghedira: Sensitivity of the meteorological model WRF-ARW to planetary
411 boundary layer schemes during fog conditions in a coastal arid region, Atmos. Res., 187, 106–127,
412 <https://doi.org/10.1016/j.atmosres.2016.12.009>, available at: <http://www.sciencedirect.com/science/article/pii/S0169809516307116>,
413 2017.
- 414 Niu, F., Li, Z., Li, C., Lee, K., and Wang, M.: Increase of wintertime fog in China: Potential impacts of weakening of the Eastern Asian
415 monsoon circulation and increasing aerosol loading, J. Geophys. Res., 115, <https://doi.org/10.1029/2009jd013484>, 2010a.

- 416 Niu, S., Lu, C., Yu, H., Zhao, L., and Lü, J.: Fog research in China: An overview, *Adv. Atmos. Sci.*, 27, 639–662,
417 <https://doi.org/10.1007/s00376-009-8174-8>, 2010b.
- 418 Rangognio, J.: Influence of aerosols on the formation and development of radiation fog, *Atmos. Chem. Phys.*, 9, 17963–18019,
419 <https://doi.org/10.5194/acpd-9-17963-2009>, 2009.
- 420 Rosenfeld, D., Meinrat O. Andreae, Asmi, A., Chin, M., and Johannes Quaas: Global observations of aerosol-cloud-precipitation-climate
421 interactions, *Rev. Geophys.*, 52, 750–808, <https://doi.org/10.1002/2013RG000441>, 2014.
- 422 Rosenfeld, D., Lohmann, U., Raga, G. B., O'Dowd, C. D., Kulmala, M., Fuzzi, S., Reissell, A., and Andreae, M. O.: Flood or drought:
423 how do aerosols affect precipitation?, *Science*, 321, 1309–1313, <https://doi.org/10.1126/science.1160606>, 2008.
- 424 Rozoff, C. M., Cotton, W. R., and Adegoke, J. O.: Simulation of St. Louis, Missouri, Land Use Impacts on Thunderstorms, *J. Appl. Mete-
425 orol.*, 42, 716–738, [https://doi.org/10.1175/1520-0450\(2003\)042<0716:SOSLML>2.0.CO;2](https://doi.org/10.1175/1520-0450(2003)042<0716:SOSLML>2.0.CO;2), 2003.
- 426 Sachweh, M. and Koepke, P.: Radiation fog and urban climate, *Geophys. Res. Lett.*, 22, 1073–1076, <https://doi.org/10.1029/95gl00907>,
427 1995.
- 428 Shepherd, J. M.: A Review of Current Investigations of Urban-Induced Rainfall and Recommendations for the Future, *Earth Interact.*, 9,
429 1–27, <https://doi.org/10.1175/ei156.1>, 2005.
- 430 Shi, C., Roth, M., Zhang, H., and Li, Z.: Impacts of urbanization on long-term fog variation in Anhui Province, China, *Atmos. Environ.*, 42,
431 8484–8492, <https://doi.org/10.1016/j.atmosenv.2008.08.002>, 2008.
- 432 Stolaki, S., Haeffelin, M., Lac, C., Dupont, J. C., Elias, T., and Masson, V.: Influence of aerosols on the life cycle of a radiation fog event.
433 A numerical and observational study, *Atmos. Res.*, 151, 146–161, <https://doi.org/10.1016/j.atmosres.2014.04.013>, 2015.
- 434 Tao, W. K., Chen, J. P., Li, Z., Wang, C., and Zhang, C.: Impact of aerosols on convective clouds and precipitation, *Rev. Geophys.*, 50,
435 6837, <https://doi.org/10.1029/2011RG000369>, 2012.
- 436 Tie, X., Huang, R., Cao, J., Zhang, Q., Cheng, Y., Su, H., Chang, D., Pöschl, U., Hoffmann, T., Dusek, U., Li, G., Worsnop, D., and
437 O'Dowd, C.: Severe Pollution in China Amplified by Atmospheric Moisture, *Sci. Rep.* 7, 15760,
438 <https://doi.org/10.1038/s41598-017-15909-1>, 2017.
- 439 Tie, X., Long, X., Li, G., Zhao, S., Cao, J., and Xu, J.: Ozone enhancement due to photo-dissociation of nitrous acid in eastern China, *At-
440 mos. Chem. Phys.*, 19, 11267–11278, <https://doi.org/10.5194/acp-19-11267-2019>, 2019.
- 441 Twomey, S. A.: The Influence of Pollution on the Shortwave Albedo of Clouds, *J. Atmos. Sci.*, 34, 1149–1154,
442 [https://doi.org/10.1175/1520-0469\(1977\)034<1149:tiopot>2.0.co;2](https://doi.org/10.1175/1520-0469(1977)034<1149:tiopot>2.0.co;2), 1977.
- 443 Wang, F., Guo, J., Zhang, J., Huang, J., Min, M., Chen, T., Liu, H., Deng, M., and Li, X.: Multi-sensor quantification of aerosol-induced
444 variability in warm clouds over eastern China, *Atmos. Environ.*, 113, 1–9, <https://doi.org/10.1016/j.atmosenv.2015.04.063>, 2015
- 445 Yan, S., Zhu, B., and Kang, H.: Long-term fog variation and its impact factors over polluted regions of East China, *J. Geophys.
446 Res.-Atmos.*, 124, 1741–1754, <https://doi.org/10.1029/2018JD029389>, 2019.
- 447 Yang, Y., Hu, X., Gao, S., and Wang, Y.: Sensitivity of WRF simulations with the YSU PBL scheme to the lowest model level height for a
448 sea fog event over the Yellow Sea, *Atmos. Res.*, 215, 253–267, <https://doi.org/10.1016/j.atmosres.2018.09.004>, 2019.
- 449 Zhang, N. and Ma, X.: Analysis of the June 2018 Atmospheric Circulation and Weather, *Meteorological Monthly*, 43, 508–512,
450 <https://doi.org/10.7519/j.issn.1000-0526.2017.04.014>, 2017. [in Chinese]
- 451 Zhang, X., Musson-Genon, L., Dupont, E., Milliez, M., and Carissimo, B.: On the Influence of a Simple Microphysics Parametrization on
452 Radiation Fog Modelling: A Case Study During ParisFog, *Bound.-Layer Meteor.*, 151, 293–315,
453 <https://doi.org/10.1007/s10546-013-9894-y>, 2014.
- 454 Zhu, B. and Guo, T.: Review of the Impact of Air Pollution on Fog, *Advances in Meteorological Science and Technology*, 6, 56–63,
455 <https://doi.org/10.3969/j.issn.2095-1973.2016.02.006>, 2016. [in Chinese]
- 456 Zhu, J., Zhu, B., Huang, Y., An, J., and Xu, J.: PM2.5 vertical variation during a fog episode in a rural area of the Yangtze River Delta,
457 China, *Sci. Total. Environ.*, 685, 555–563, <https://doi.org/10.1016/j.scitotenv.2019.05.319>, 2019.

459 Table 1. Summary of major parameterization schemes.

Scheme	Option
Boundary layer	YSU
Longwave radiation	RRTM
Shortwave radiation	New Goddard
Microphysics	Morrison
Surface layer	MM5 similarity
Land surface	Noah
Urban surface	Urban canopy model
Gas phase chemistry	CBMZ
Aerosol chemistry	MOSAIC (4-bin)
Aerosol-cloud and aerosol-radiation interactions	All turned on
Aerosol activation	Abdul-Razzak and Ghan (2002)

460

461

462

Table 2. Settings of sensitive experiments. "N" represents no changes.

Case name	Description	Underlying surface	Anthropogenic emission
u0e0	base condition	N	N
u3e0	urbanization condition	the 11x13 grid centered on SX is replaced by urban surface	N
u0e3	polluted condition	N	the 11x13 grid centered on SX is replaced by the emis- sion of Hefei downtown
u3e3	urbanization and polluted condition	same as u3e0	same as u0e3

Effect	Description
u3e0-u0e0	urbanization effect
u0e3-u0e0	aerosol effect
u3e3-u0e0	urbanization and aerosol effect

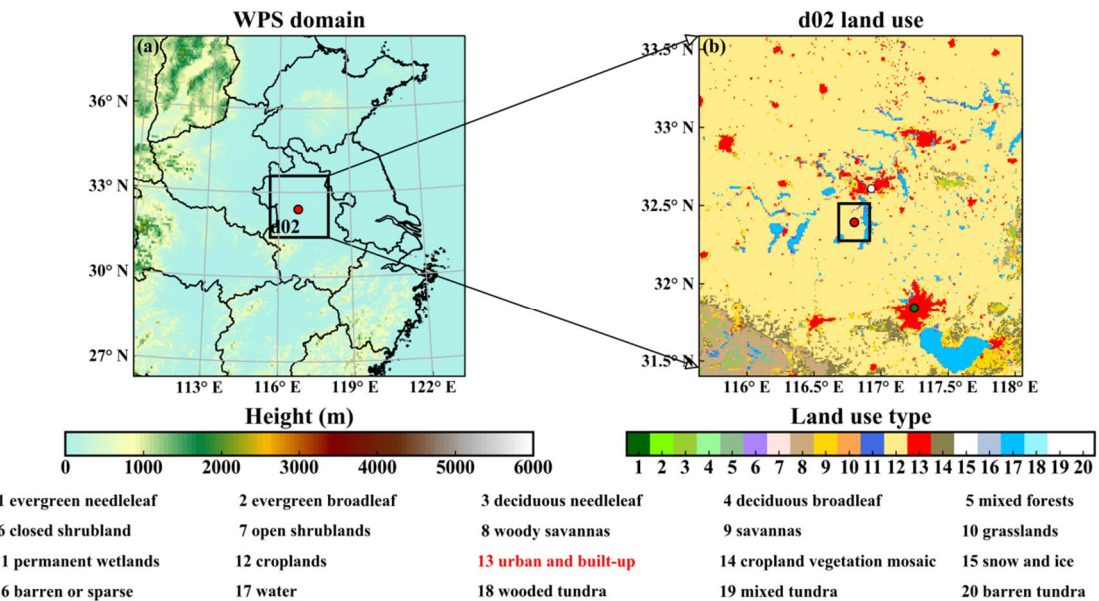
463

464

465

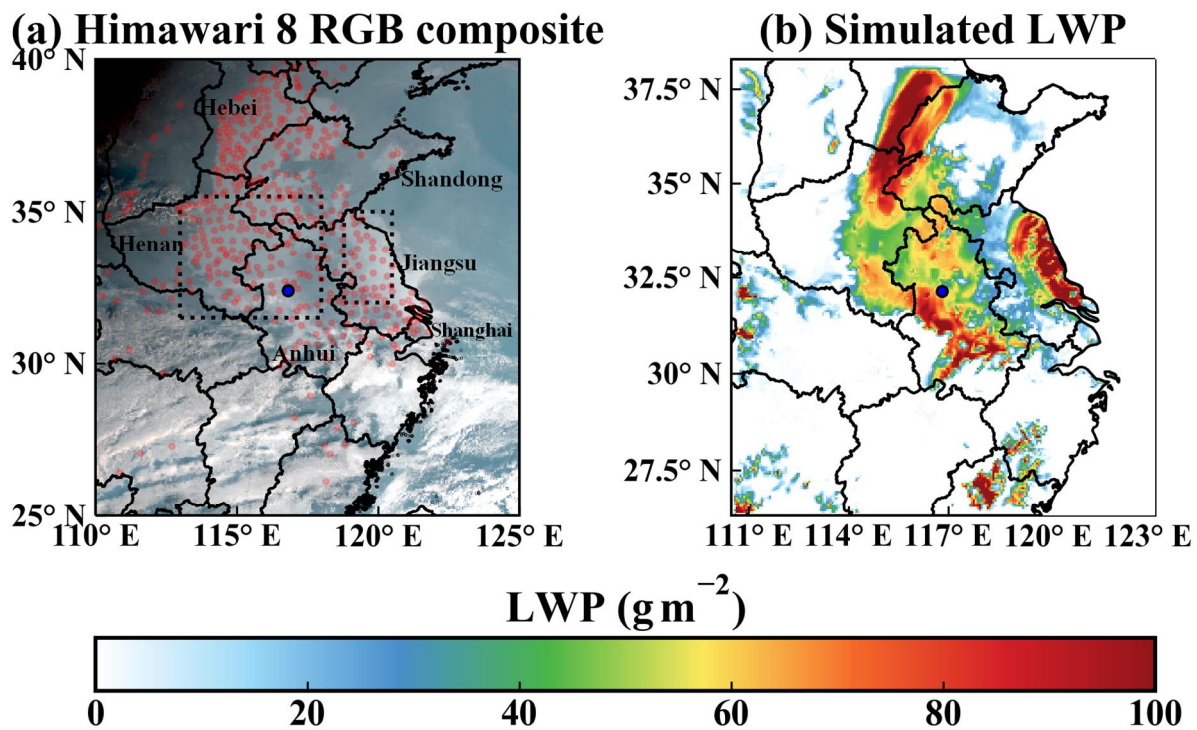
466

467



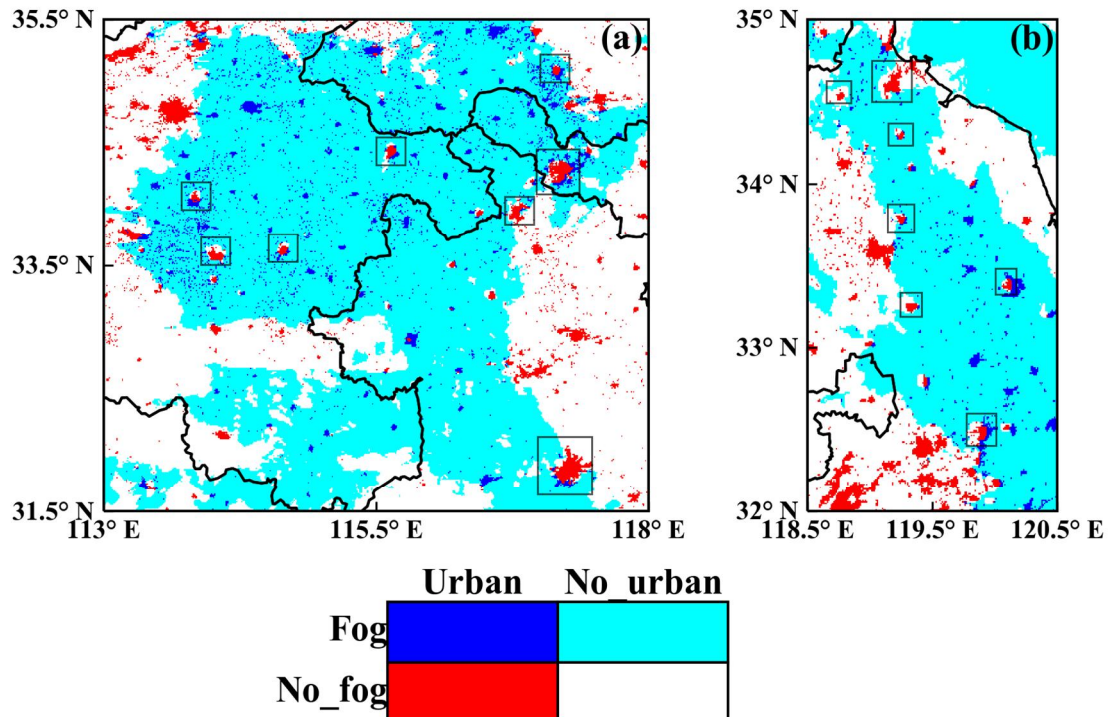
469

470 Figure 1. (a) The WRF domain overlaid with terrain height. (b) The land use distribution of domain d02. The green dot
 471 is Hefei, the capital of Anhui Province. The white dot is Huainan. The two red dots are the SX site. The land use and
 472 emissions of the 22 km×26 km black box in the center of (b) will be altered in the sensitivity experiments.
 473

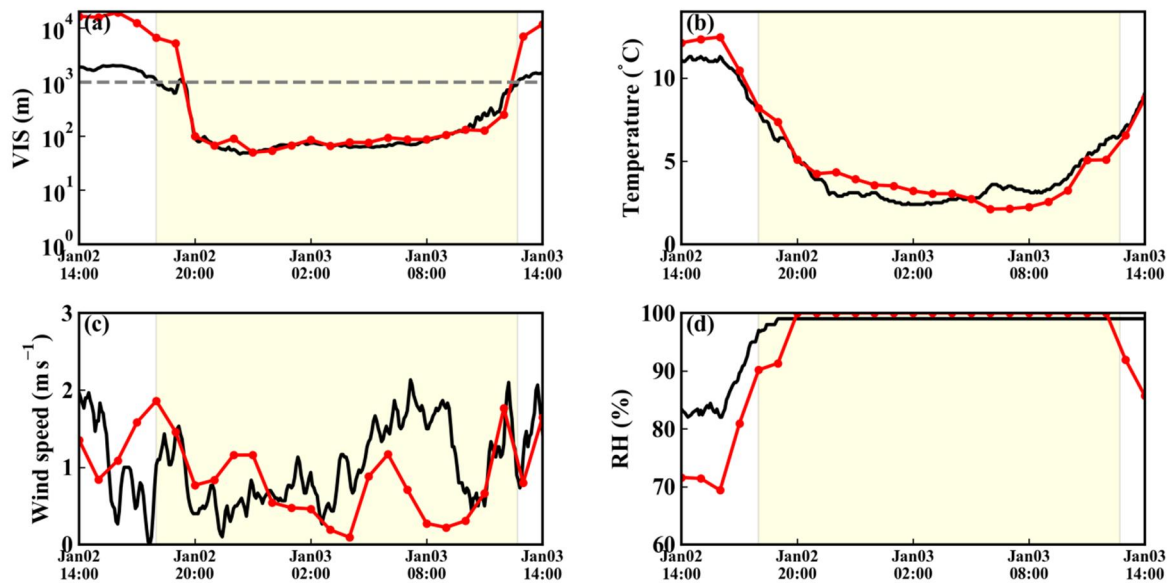


476 Figure 2. The performance of the simulated fog zone at 08:00 03 January 2017. (a) Himawari 8 RGB composite cloud
 477 image overlaid with the MICAPS observation sites (light red dots) at which fog was observed (relative humidity > 90 %
 478 and VIS < 1 km). (b) Simulated LWP distribution. Only LWC below 1500 m are integrated. The blue dots are the SX
 479 site. The two dashed rectangles in (a) are the subregions of interest in Fig. 3.

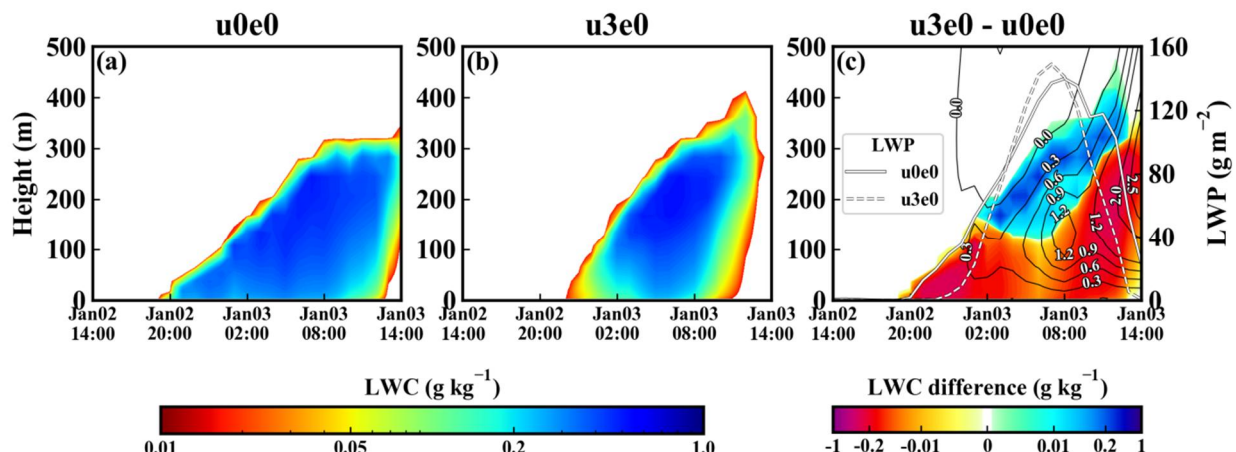
480



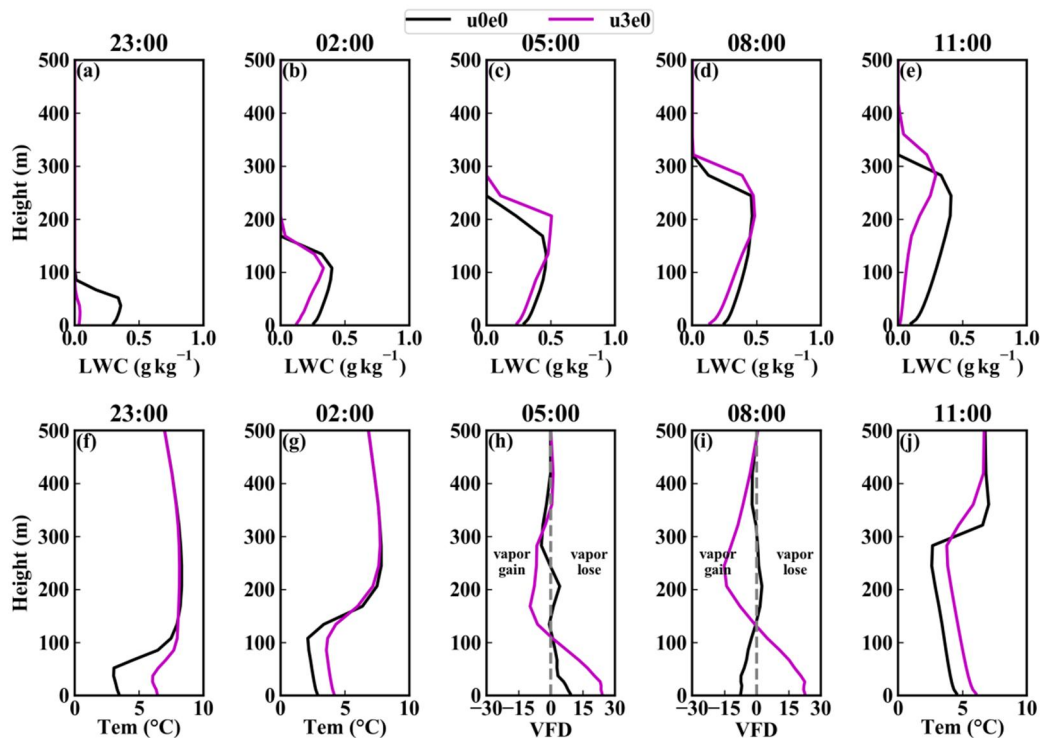
483 Figure 3. Two sub-regions (a and b) with obvious fog holes on the Himawari 8 image at 11:00 03 January 2017. The
 484 fog zone, which is represented by albedo > 0.45 (at $0.64 \mu\text{m}$) and brightness temperature $> 266 \text{ K}$ (at $12.4 \mu\text{m}$) (Di
 485 Vittorio et al., 2002), is marked with cold colours (blue or cyan). The urban areas are marked with blue or red. The red
 486 and white pixels surrounded or semi-surrounded by cold colours are fog holes, and among these pixels, the red pixels
 487 indicate the fog holes over urban areas. Some of the cities with fog holes are marked by rectangles.
 488



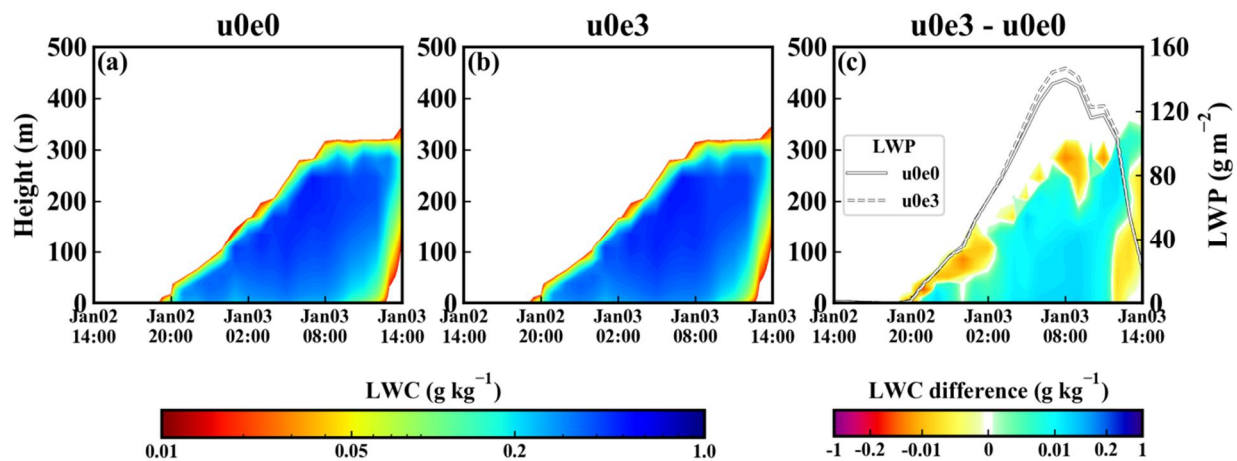
491 Figure 4. The performance of the simulated meteorological parameters at the SX site. (a) VIS. (b) air temperature. (c)
 492 10-minute average wind speed. (d) Relative humidity (RH). The red dotted lines represent the model results, and the
 493 black lines are the observations. The fog period ($\text{VIS} < 1 \text{ km}$ and $\text{RH} > 90\%$) is shaded with light yellow.
 494

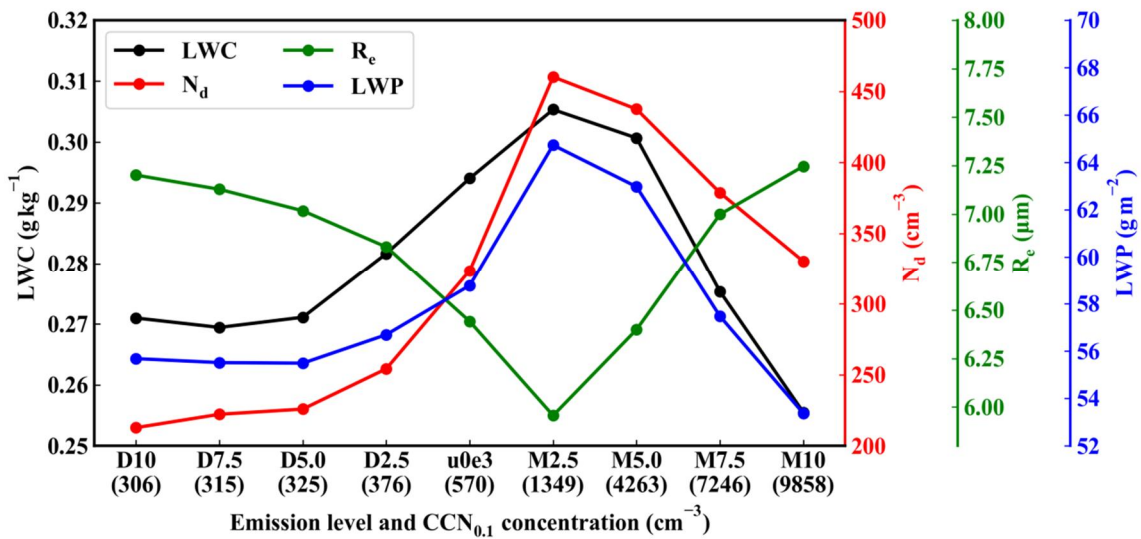


497 Figure 5. Time-height distribution of the LWC (g kg^{-1}) in (a) u0e0 and (b) u3e0, and (c) is the urbanization effect (u3e0
498 minus u0e0) on LWC. The two white curves in (c) are the LWP. The black contour lines in (c) are the difference of
499 vertical velocity (cm s^{-1}) (u3e0 minus u0e0). Only the lines after 00:00 are shown for clarity.

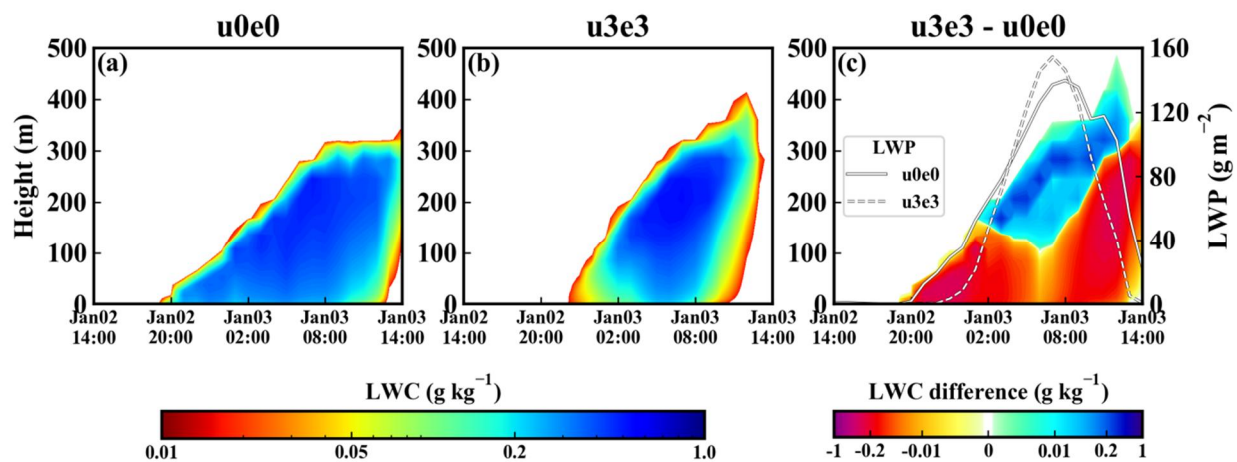


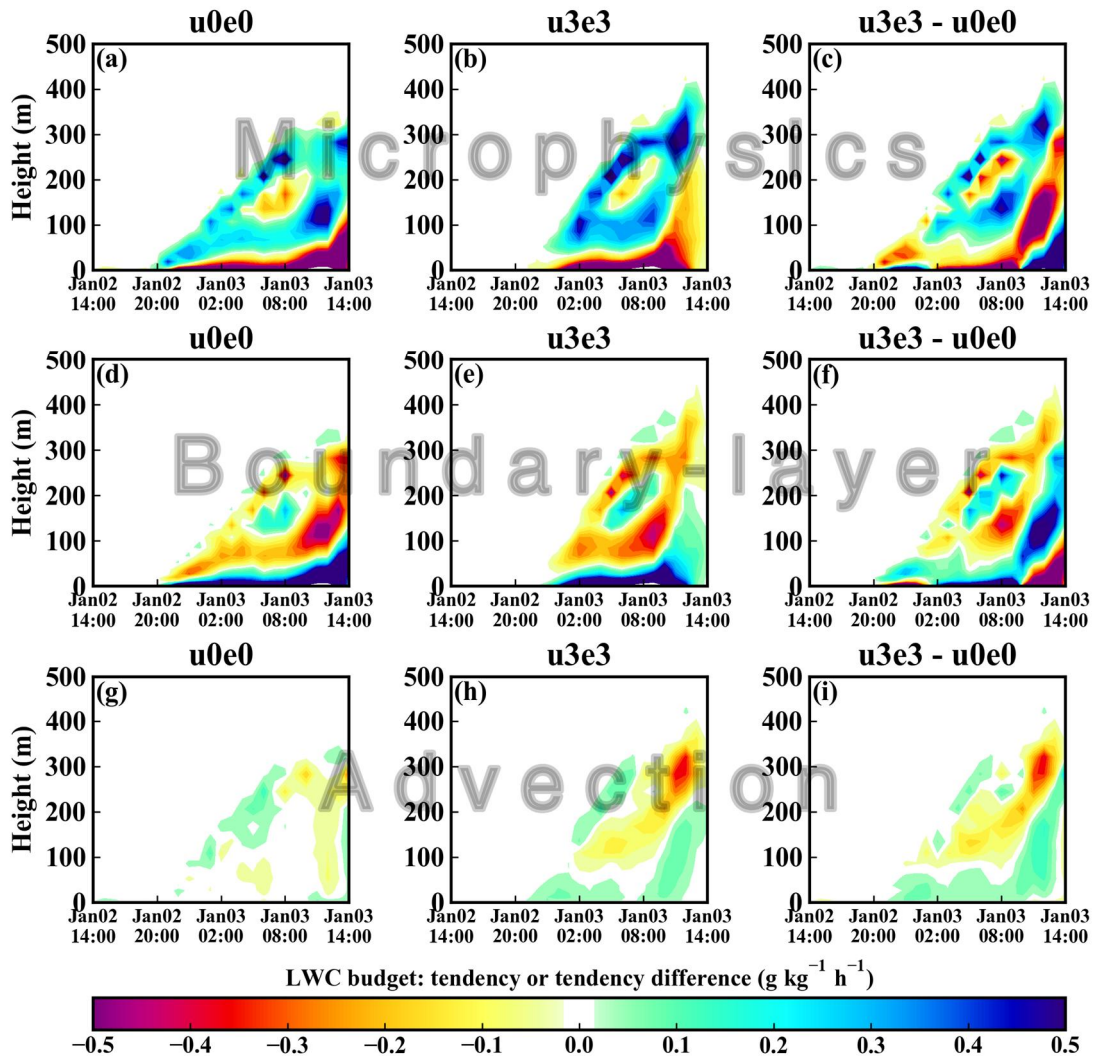
503 Figure 6. Profiles of the LWC (first row), temperature (Tem) (f, g, j) and vertical vapour flux divergence (VFD) (h, i)
 504 (g h⁻¹ m⁻²·hPa⁻¹) in u0e0 and u3e0 at different times.
 505

508 Figure 7. Similar to Fig. 5, but for the aerosol effect ($u0e3$ minus $u0e0$).

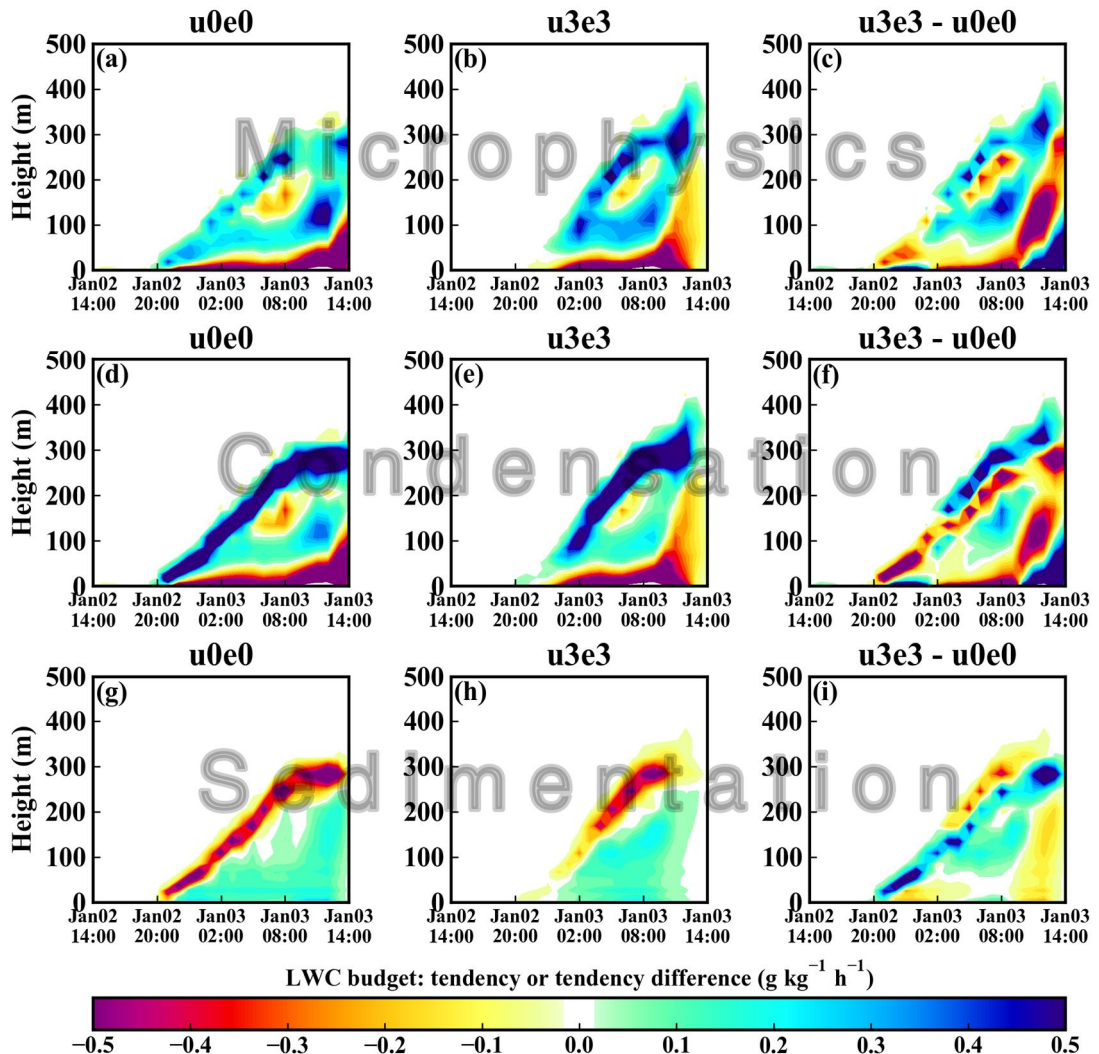


512 Figure 8. Relationships of the microphysical parameters (LWC, N_d , R_e and LWP) with emission level and $\text{CCN}_{0.1}$ concentrations. These parameters are the time-height averages (time average for the LWP) in fog.
 513
 514

517 Figure 9. Similar to Fig. 5, but for the combined effect of urbanization and aerosols (u3e3 minus u0e0).
518



521 Figure 10. The combined effect of urbanization and aerosols ($u3e3$ minus $u0e0$) on various items of the LWC budget.
 522 The three rows are the **hourly** tendencies ($\text{g kg}^{-1} \text{h}^{-1}$) of the microphysical, boundary layer, and advection processes.
 523



526 Figure 11. The combined effect of urbanization and aerosols ($u3e3$ minus $u0e0$) on various items of the microphysical
 527 | tendency. The three rows are the **hourly** tendencies ($\text{g kg}^{-1} \text{h}^{-1}$) of the microphysical, condensation/evaporation, and
 528 | sedimentation processes.